NIH Public Access
Author Manuscript
J Phys Chem B. Author manuscript; available in PMC 2011 September 15.

Published in final edited form as:
J Phys Chem B. 2010 February 4; 114(4): 1632–1637. doi:10.1021/jp909048f.

Fluctuations of water near extended hydrophobic and hydrophilic surfaces

Amish J. Patel, **Patrick Varilly**, and **David Chandler**
Department of Chemistry, University of California, Berkeley, California 94720

Abstract

We use molecular dynamics simulations of the SPC-E model of liquid water to derive probability distributions for water density fluctuations in probe volumes of different shapes and sizes, both in the bulk as well as near hydrophobic and hydrophilic surfaces. Our results are obtained with a biased sampling of coarse-grained densities that is easily combined with molecular dynamics integration algorithms. Our principal result is that the probability for density fluctuations of water near a hydrophobic surface, with or without surface-water attractions, is akin to density fluctuations at the water-vapor interface. Specifically, the probability of density depletion near the surface is significantly larger than that in bulk, and this enhanced probability is responsible for hydrophobic forces of assembly. In contrast, we find that the statistics of water density fluctuations near a model hydrophilic surface are similar to that in the bulk.

Introduction

According to theory, fluctuations of water density on sub-nanometer length scales obey Gaussian statistics,[1–3] while those on larger length scales deviate significantly from this behavior.[4] The deviations at large length-scales reflect the fact that water at standard conditions lies close to water-vapor coexistence.[4,5] A large enough repellent surface can therefore induce the formation of a water-vapor-like interface, and as such, the probability of water depletion is enhanced near such a surface. In particular, the presence of this liquid-vapor-like interface facilitates large fluctuations in its vicinity compared to that in the bulk. This perspective is at the heart of current ideas about hydrophobic effects.[6,7] In this paper, we use molecular simulations to further examine the validity of this perspective. We demonstrate marked similarities between water-vapor interfaces and water-oil interfaces for large enough oily surfaces with low radii of curvature.

The fact that a purely repulsive hydrophobic surface induces the formation of a vapor-liquid-like interface is well-established.[4,8–10] Dispersive attractions between the hydrophobic surface and water can mask this effect, as the attractions move the interface to a mean position immediately adjacent to the hydrophobic surface. This removes any significant presence of vapor on average.[10–13] As a result, it is difficult to detect the presence of a water-vapor-like interface by considering only the mean behavior of water density profiles. Rather, the presence of this interface is more directly reflected in fluctuations away from those profiles,[6,14–19] which motivates our focus here on the statistics of these density fluctuations.

Several groups have studied the statistics of these fluctuations.[3,20,21] This paper is distinguished from this earlier work by the fact that we report the statistics of large length-scale fluctuations, which are expected[4] to be fundamentally different from the small length-

Correspondence to: David Chandler.

NIH-PA Author Manuscript
NIH-PA Author Manuscript
NIH-PA Author Manuscript

NIH-PA Author Manuscript

NIH-PA Author Manuscript

NIH-PA Author Manuscript

scale fluctuations studied in the earlier work. Large length-scale water density fluctuations control pathways for assembling hydrophobically stabilized structures.4,22–29

The central quantity to be examined is the probability for finding N water molecules in a sub-volume v, $P_v(N)$. Hummer and Pratt and their co-workers introduced the idea of studying this function as a route to understanding solvation.3,20,30,31 In pure solvent, large length-scale fluctuations are very rare, but these are the fluctuations of interest here. Therefore, to obtain reasonable statistical information, we must employ some form of biased non-Boltzmann sampling.32,33 The simulation setup and system details are described in the next section, after which we explain the specific sampling method that we employ. Results are then presented, beginning with those for the length-scale dependence of fluctuations in bulk water, followed by a discussion of the effect of dispersive attractions between the water molecules and a hydrophobic surface. Finally, we contrast fluctuations near a hydrophobic surface with those near a hydrophilic surface.

Our results are qualitatively consistent both with the Lum-Chandler-Weeks (LCW)4 theory for the length-scale dependence of hydrophobic effects and with recent computer simulation studies.18,34 This present work, however, is the first publication of quantitative computer simulation data on the nature of water density fluctuations that deviate far from the mean in an atomistic model of water.35 As such, it is the first test with an atomistic model of the underlying assumptions from which the LCW theory derives. Further, as a matter of technical interest, the numerical technique we use to determine reliable distributions for rare fluctuations is new and may prove useful in other contexts.

Simulation Models

For the purposes of studying hydrophobic effects and juxtaposing hydrophobic and hydrophilic solvation, it is most important that the liquid be close to liquid-vapor equilibrium with a substantial surface tension, that it has a high dielectric constant and small compressibility, and that its molecules typically arrange with local tetrahedral order.6 There are many models that could be used to satisfy these criteria. We have used the SPC-E model. 36 Given the many commonalities between behaviors we elucidate here and those found with models as simple as the lattice-gas,19,23 it seems unlikely that our findings would change significantly if we changed to another standard atomistic model of water.

Density fluctuations of SPC-E water in the canonical ensemble at 298K can be quantified using the LAMMPS molecular dynamics (MD) simulation package.37 Specifically, we evaluate the probability, $P_v(N)$, of finding N water oxygens in a probe volume of interest, v. A straightforward canonical ensemble simulation, with an average water density, $\rho = 1$ g/cm^3, would suppress large density fluctuations. To avoid this suppression, a particle-excluding field is introduced on one surface of the simulation box, with the box large enough that the net density is less than the bulk liquid density. Through this construction38,39 we ensure that the bulk liquid remains in the center of the box, that it is at coexistence with its vapor phase, and that a free liquid-vapor interface acts as a buffer in the event of a large density fluctuation. Solutes are placed near the center of the box, deep within the bulk liquid and far from the free water-vapor interface.

To model a hydrophilic solute, we consider water molecules within a particular sub-volume of bulk water, specifically a sub-volume of dimensions $3 \times 24 \times 24$ Å^3. Taking a configuration of equilibrated bulk liquid, we immobilize those water molecules that are within this sub-volume. The immobilized molecules are then the solute. Its surface is unlikely to disrupt the hydrogen bond network of the neighboring solvent because the surface is made up of fixed water molecules in a configuration that is typical of bulk water.

NIH-PA Author Manuscript

NIH-PA Author Manuscript

NIH-PA Author Manuscript

Indeed, to the extent that fluctuations in water structure are unimportant, there is no cost in free energy to solvate this solute. In this sense, it is an ideal hydrophilic solute.

To model a hydrophobic solute, we replace the fixed waters in our model of a hydrophilic solute with methane-like oily particles. These oily particles are uncharged and interact with the surrounding solvent water molecules via a standard water-methane Lennard-Jones potential.40 The resulting potential energy field expels water from the volume occupied by the solute. It also attracts water with dispersive interactions. The solute constructed in this way and a typical configuration of solvent water are shown in Fig. 1.

In order to study the effect of dispersive attractions on water-density fluctuations, the Lennard-Jones (LJ) pair potential between the hydrophobic solute and the solvent is split into repulsive and attractive parts using the Weeks-Chandler-Andersen (WCA) prescription.41 The role of attractions can then be examined systematically with a scaling parameter λ,

$$u_\lambda(r)=u_0(r)+\lambda\Delta u(r), \tag{1}$$

where $u_0(r)$ and $\Delta u(r)$ are the WCA repulsive and attractive branches of the LJ potential, respectively, σ = 3.905Å and ε = 0.118Kcal/mol were used as the LJ parameters for the oily particles,40 and Lorentz-Berthelot mixing rules were used to obtain water-solute interaction parameters.

Umbrella sampling

Since we have chosen molecular dynamics to probe our system, it is convenient to use a biasing umbrella potential that produces continuous forces. The potential we use is a function of the entire set of water oxygen coordinates: $\{\mathbf{r}_i\}$, $i = 1, 2, \ldots M$. The number of molecules, N, in a specific volume, v, is not a continuous function of $\{\mathbf{r}_i\}$, but the biasing potential we use to influence this number is a continuous function of these variables. In particular, we focus on the coarse-grained particle number:

$$\widehat{N}(\{\mathbf{r}_i\},\mathrm{v})=\int d\mathbf{r}\sum_{i=1}^{M}\Phi(\mathbf{r}-\mathbf{r}_i)h_\mathrm{v}(\mathbf{r}), \tag{2}$$

where $h_\mathrm{v}(\mathbf{r}) = 1$ or 0, depending on whether or not $\mathbf{r}$ is in volume v, $\mathbf{r}$ has Cartesian coordinates x, y, z, and

$$\Phi(\mathbf{r})=\varphi(x)\varphi(y)\varphi(z) \tag{3}$$

with φ(x) being a normalized, truncated and shifted Gaussian-like distribution,

$$\varphi(x)\propto[\exp(-x^2/2\xi^2)-\exp(-r_\mathrm{c}^2/2\xi^2)]\theta(r_\mathrm{c}-|x|). \tag{4}$$

The proportionality constant is the normalization constant, θ(x) is the Heaviside step function, and we have chosen the coarse-graining length ξ to be 0.1Å and the cut-off length r_c to be 0.2Å.

In the limit $\xi \to 0$, the dynamical variable $\tilde{N}(\{\mathbf{r}_i\},\mathrm{v})$ is the actual number of water molecules in the volume v. But for finite ξ, $\tilde{N}(\{\mathbf{r}_i\};\mathrm{v})$ is a continuous and differentiable function of $\{\mathbf{r}_i\}$. We construct the biasing potential with this variable. In particular, we let

NIH-PA Author Manuscript

NIH-PA Author Manuscript

NIH-PA Author Manuscript

$$U(\{\mathbf{r}_i\};\kappa,\eta)=\frac{\kappa}{2}[\widehat{N}(\{\mathbf{r}_i\},\mathrm{v})-\eta]^2, \tag{5}$$

where κ is a positive constant. We have found it convenient to use κ = 0.25 kcal/mol. Simulating our system in the presence of this umbrella potential allows us to bias the system towards configurations with $\tilde{N}(\{\mathbf{r}_i\},\mathrm{v})$ values near η. When η differs substantially from the mean value for the dynamical variable, these configurations will be very improbable in the unperturbed system. Nevertheless, these configurations can be accessed reversibly through a series of simulations that slowly change the control variable η.

By influencing the coarse-grained number of particles in the probe volume, the control variable η also influences the actual number of water molecules in that volume. We have picked a small value of the coarse graining length ξ to ensure that the latter influence is significant. As a result, with a series of simulations with different values of η, histograms for both the coarse-grained number and the actual number can be collected and then unbiased and stitched together within the framework of the weighted histogram analysis method (WHAM).[42–44] This procedure yields the joint distribution function that the coarse grained particle number, $\tilde{N}(\{\mathbf{r}_i\},\mathrm{v})$, has value $\tilde{N}$ and the actual particle number is N. The joint distribution, $P_\mathrm{v}(N,\tilde{N})$, can then be integrated to give the distribution of interest, $P_\mathrm{v}(N)$.[45,46] With $P_\mathrm{v}(N)$ known, the free energy of solvation of a "hard" solute or cavity of volume v, $\Delta\mu_\mathrm{v}$, is also known because[3,46]

$$\beta\Delta\mu_\mathrm{v}=-\ln P_\mathrm{v}(0) \tag{6}$$

where $k_\mathrm{B}\beta = 1/\mathrm{T}$ is inverse temperature and k_B is Boltzmann's constant. This formula holds irrespective of where the probe volume is placed, whether close to or far from a solute. The free energy of solvation depends, of course, on the location, shape and size of v, and we explore aspects of this dependence with the results reported below.

Results

Length-scale dependence of density fluctuations in bulk water

In Fig. 2, we show results for $P_\mathrm{v}(N)$ in different probe volumes in bulk water. Because $P_\mathrm{v}(N)$ is Gaussian for molecularly sized probe volumes,[3] we present these results in comparison with Gaussians of the same mean, $\langle N\rangle_\mathrm{v}$, and the same variance, $\langle(\delta N)^2\rangle\mathrm{v}$. For small deviations from the mean, $P_\mathrm{v}(N)$ is essentially Gaussian, and for small volumes v, only small deviations from the mean N are possible. For large v, however, the wings of the distribution differ markedly from Gaussian for small N.

In pure water, the chance of observing these deviations is negligible, less than one part in many powers of ten. On the other hand, these deviations become accessible and even dominant near a sufficiently large and repellent solute particle. In particular, while the free energy to reduce N, namely $-k_\mathrm{B}T\ln[P_\mathrm{v}(N)]$ is parabolic near the mean, it can vary linearly or sub-linearly with N in the wings of the distribution for a large enough volume v. See Fig. 2a for the case of a large cubic probe volume. The introduction of a perturbing potential, perhaps due to the presence of another solute, introduces a potential energy that scales linearly with N. If $-k_\mathrm{B}T\ln[P_\mathrm{v}(N)]$ were parabolic for all N, the addition of such a potential energy would simply shift the parabola to a different mean. However, when $-k_\mathrm{B}T\ln[P_\mathrm{v}(N)]$ varies linearly or sub-linearly with N in the wings of the distribution, a perturbing potential can favor low N to the point where low values become the most probable values. This type

NIH-PA Author Manuscript

NIH-PA Author Manuscript

NIH-PA Author Manuscript

of shift in the distribution, which can occur only for large v, is responsible for many large length-scale hydrophobic effects.4

In the case of the large but thin rectangular volume considered in Fig. 2a, the wings of $P_v(N)$ also exhibit deviations from Gaussian behavior.47 In this case, however, the distribution lies below the Gaussian. The differences between the distribution for the large cubic volume and that for the large thin volume reflects interfacial dominance of hydrophobic solvation in the large length-scale regime. Namely, the surface area of large thin volume is larger than that of the large cubic volume, and in the large length-scale regime, $\Delta\mu_v \approx A_v \tilde{\gamma}$. Here, A_v is the surface area52 of the volume v, and $\tilde{\gamma}$ is a free energy per unit area that depends weakly upon v. Figure 2b illustrates the accuracy of this approximation for the length scale regime considered. (The value of $\tilde{\gamma}$ is of the order of but smaller than the liquid-vapor surface tension, γ, as is expected for the size of volumes considered.49,51) Thus, the probabilities for emptying the large cubic and large thin probe volumes differ by about 25 orders of magnitude largely because of differing free energies of interface formation.

To elaborate, consider the solvation energy for the cavity v, relative to that of *n* independent smaller voids, say $\delta v = 3 \times 6 \times 6$ Å^3:

$$\Delta\Delta\mu_v = \Delta\mu_v - n\Delta\mu_{\delta v}. \quad (7)$$

Here, $\Delta\mu_{\delta v}$ denotes the solvation free energy for a single independent smaller void δv and the net volume v is composed of n such voids, i.e., $n = v/\delta v$. $\Delta\Delta\mu_v$ is the free energy of hydrophobic assembly – the change in free energy as a result of assembling the cavity v from the *n* separated components. In the small length-scale regime, the net solvation energy would be $n\Delta\mu_{\delta v}$, and this free energy would be a good approximation to the value of $-k_B T \ln[P_{n\delta v}(0)]$, to the extent that $P_{n\delta v}(N)$ is the Gaussian distribution centered at the mean value of *N*.53,54 As such, the extent to which $P_v(N)$ deviates from the corresponding Gaussian, and the extent to which the resultant $\Delta\Delta\mu_v$ is non-trivial, is the extent to which large length-scale effects are important.6 Figure 2a shows that these effects cause a favorable driving force to assemble the smaller voids into a cubic geometry, and they cause an unfavorable driving force to assemble the smaller voids into a thin geometry.

The fat tail of $P_v(N)$ in the regime of small *N*, responsible for the favorable hydrophobic driving force of assembly, manifests the formation of a liquid-vapor interface. The existence of such tails are expected for large enough probe volumes in any liquid close to liquid-vapor phase coexistence,4,55 and they have been found in simulations of various models.56,57 Figure 2, however, provides the first demonstration of these tails in an atomistic model of bulk liquid water. Figure 2 also provides the first such demonstration that fat tails will disappear when a large volume is reshaped into a sufficiently constraining geometry.

Water near hydrophobic surfaces and the effect of dispersive attractions

Figure 3 shows normalized mean densities as a function of the distance, *x*, from the center of the idealized large flat hydrophobic solute (see Fig. 1). Several strengths of dispersive attractions between the solute and water are considered. See Eq. (1). For $\lambda = 0$, the mean density profile is sigmoidal, suggestive of a vapor-liquid interface. However, addition of a small amount of attraction results in a qualitatively different density profile. For $\lambda = 0.4$, there is a maximum in the density profile accompanied by layering. Further increasing the attractions leads to a more pronounced maximum and layering. This behavior is in accord with the qualitative predictions of LCW theory.10 Nevertheless, contrary to these predictions, it has been suggested that a layered density profile implies an absence of a liquid-vapor-like interface near an extended hydrophobic surface with dispersive attractions

NIH-PA Author Manuscript

NIH-PA Author Manuscript

NIH-PA Author Manuscript

to water.11,58 Confusion on this point seems to reflect a singular focus on the mean density, but the mean by itself is not an obvious indicator of liquid-vapor-like interfaces. Interfaces are relatively soft so that a weak perturbation can affect the location of the interface and thus the mean density profile while not destroying the interface.57 In other words, in order to fully appreciate the effect that a hydrophobic solute has on the surrounding solvent, one should look at both the mean density and the density fluctuations.6

The statistics for these fluctuations can be obtained from the distribution of particle numbers in suitably chosen probe volumes. Figure 4a shows $P_v(N)$ distributions for the thin rectangular probe volume v=(3 × 24 × 24) Å^3 placed between x = 5Å and x = 8Å. With this position, there is no overlap between solute particles and water molecules in v, as inferred from their van der Waals' radii. The distributions for $\lambda = 0$ and $\lambda = 0.4$ are similar, with the probability of density depletion slightly lower for the latter case, but still significantly higher than that in the bulk.

The free energy to empty this probe volume adjacent to the large hydrophobic solute with $\lambda = 0.4$ is 57 k_BT, whereas the free energy to empty this same v when it is in bulk and far from the hydrophobic surface is 147 k_BT. See Fig. 4b. This large difference in free energies is due to interface formation. In Fig. 3, the presence of a liquid-vapor-like interface is evident in the mean density of solvent near the extended hydrophobic solute with $\lambda = 0$. $P_v(0)$ for v adjacent to the solute is then essentially the probability to move the interface outwards by 3Å from $x \simeq 5$ Å to $x \simeq 8$ Å. The free energetic penalty, $\Delta\mu_v$, for this process is 48k_BT. See Fig. 4b. The corresponding $\Delta\mu_v$ for $\lambda = 0.4$ is 57k_BT, only a 9k_BT increase on turning the attractions on to $\lambda = 0.4$ and as much as 90k_BT less than that required to form interfaces.

Hence, while the presence of a mean density maximum and layering at $\lambda = 0.4$ might lead one to question the presence of a liquid-vapor-like interface, the probabilities for fluctuations in density and the ease with which a volume near the hydrophobic surface can be vacated leaves no doubt as to its presence. Further, the presence of this interface is responsible for the hydrophobic force of assembly. In particular, because large solvent density fluctuations are more likely adjacent to a hydrophobic surface than in bulk, the free energy cost to reorganize solvent and thus solvate a cavity is significantly lower than that in bulk. Figure 4b shows that this effect is dominant until solute-solvent attractions are nearly 3 times the value of typical dispersive attractions between hydrophobic solutes and water.

Fluctuations near hydrophobic and hydrophilic surfaces

Figure 5a shows $P_v(N)$ for the probe volume v = (3 × 24 × 24) Å^3 next to the hydrophobic solute ($\lambda = 1$), and compares it with that for the probe volume next to the hydrophilic solute. Near the hydrophilic solute, the probability is nearly identical to the $P_v(N)$ for v in the bulk. On the other hand, near the hydrophobic solute, the tail in the probability and thus the probability of density depletion, is significantly higher than that in bulk.

Figure 5b shows the solvation free energy, $\Delta\mu_v$, of the probe cavity as a function of the distance between the center of the solute and the center of the cavity volume. For the cavity v near the hydrophilic solute, this free energy is essentially equal to that for the cavity v in the bulk. On the other hand, $\Delta\mu_v$ for the cavity near the hydrophobic solute increases monotonically as the cavity is moved away from the solute and eventually plateaus at its bulk value. The variation of this free energy with respect distance from the solute shows that the considered hydrophobic surface affects density fluctuations in the water at a distance of up to ~ 10Å. This behavior is in agreement with recent simulation studies, reporting the free energy of solvating a molecularly sized WCA cavity near hydrophobic surfaces18 and also the potential of mean force for bringing two hydrophobic plates close together.34

NIH-PA Author Manuscript

NIH-PA Author Manuscript

NIH-PA Author Manuscript

Summary

With the results presented above, we have shown that: **1**. For a typical large volume in pure water, $P_V(N)$ exhibits fat tails at small N. These tails, never before demonstrated in an atomistic model of liquid water, manifest the formation of liquid-vapor interfaces. **2**. For large volumes that do not exhibit these tails in bulk water, the solvation behavior is still governed by interfacial energetics, and $P_V(N)$ does exhibit fat tails at small N when these volumes are placed adjacent to a hydrophobic surface. **3**. These tails do not appear adjacent to hydrophilic surfaces. **4**. These tails, reflecting relative softness of a liquid-vapor interface and enhanced probability of water depletion, imply that the free energy of a cavity adjacent to a hydrophobic surface is more favorable than that of a cavity in bulk.

These results bear directly on nano-scale assembly where two hydrophobic surfaces may approach each other, and at least one of these surfaces is large enough to induce the formation of the soft liquid-vapor-like interface. At a particular separation, the liquid between them will be sufficiently destabilized to make drying and hydrophobic assembly kinetically accessible. In contrast, density fluctuations near a hydrophilic surface are identical to those in the bulk and the vapor phase is not stabilized by the presence of a hydrophilic surface. Hydrophobic and hydrophilic surfaces thus differ fundamentally in the way they affect the fluctuations of water molecules in their proximity. It is not the mean density, but rather the statistics of fluctuations that is most important.

Acknowledgments

We would like to acknowledge Adam Willard for helpful discussions as well as Shekhar Garde and Gerhard Hummer for sharing their work on similar issues prior to publication. This research was supported by NIH grant no. R01-FM078102.

References

1. Pratt LR, Chandler D. J. Chem. Phys. 1977; 67:3683–3704.
2. Chandler D. Phys. Rev. E. 1993; 48:2898–2905.
3. Hummer G, Garde S, Garcia AE, Pohorille A, Pratt LR. Proc. Nat. Acad. Sci. 1996; 93:8951–8955. [PubMed: 11607700]
4. Lum K, Chandler D, Weeks JD. J. Phys. Chem. B. 1999; 103:4570–4577.
5. Hilfer R, Biswal B, Mattutis HG, Janke W. Phys. Rev. E. 2003; 68:046123.
6. Chandler D. Nature. 2005; 437:640–647. [PubMed: 16193038]
7. Berne BJ, Weeks JD, Zhou R. Ann. Rev. Phys. Chem. 2009; 60:85–103. [PubMed: 18928403]
8. Stillinger FH. J. Solution Chem. 1973; 2:141–158.
9. Wallqvist A, Berne BJ. J. Phys. Chem. 1995; 99:2893–2899.
10. Huang DM, Chandler D. J. Phys. Chem. B. 2002; 106:2047–2053.
11. Choudhury N, Pettitt BM. J. Am. Chem. Soc. 2007; 129:4847–4852. [PubMed: 17385863]
12. Choudhury N, Pettitt BM. Mol. Sim. 2005; 31:457–463.
13. Ashbaugh HS, Paulaitis ME. J. Am. Chem. Soc. 2001; 123:10721–10728. [PubMed: 11674005]
14. Athawale MV, Goel G, Ghosh T, Truskett TM, Garde S. Proc. Nat. Acad. Sci. 2007; 104:733–738. [PubMed: 17215352]
15. Ball P. Chem. Phys. Phys. Chem. 2008; 9:2677–2685.
16. Mittal J, Hummer G. Proc. Nat. Acad. Sci. 2008; 105:20130–20135. [PubMed: 19074279]
17. Sarupria S, Garde S. Phys. Rev. Lett. 2009; 103:037803. [PubMed: 19659321]
18. Godawat R, Jamadagni SN, Garde S. Proc. Nat. Acad. Sci. 2009; 106:15119–15124. [PubMed: 19706896]
19. Willard AP, Chandler D. Faraday Disc. 2009; 141:209–220.

NIH-PA Author Manuscript NIH-PA Author Manuscript NIH-PA Author Manuscript

20. Garde S, Hummer G, Garcia AE, Paulaitis ME, Pratt LR. Phys. Rev. Lett. 1996; 77:4966–4968. [PubMed: 10062679]
21. Garde S, Khare R, Hummer G. J. Chem. Phys. 2000; 112:1574–1578.
22. ten Wolde PR, Chandler D. Proc. Nat. Acad. Sci. 2002; 99:6539–6543. [PubMed: 11983853]
23. Willard AP, Chandler D. J. Phys. Chem. B. 2008; 112:6187–6192. [PubMed: 18229916]
24. Huang X, Margulis CJ, Berne BJ. Proc. Nat. Acad. Sci. 2003; 100:11953–11958. [PubMed: 14507993]
25. Zhou R, Huang X, Margulis CJ, Berne BJ. Science. 2004; 305:1605–1609. [PubMed: 15361621]
26. Liu P, Huang X, Zhou R, Berne BJ. Nature. 2005; 437:159–162. [PubMed: 16136146]
27. Giovambattista N, Rossky PJ, Debenedetti PG. Phys. Rev. E. 2006; 73:041604.
28. Krone MG, Hua L, Soto P, Zhou R, Berne BJ, Shea J-E. J. Am. Chem. Soc. 2008; 130:11066–11072. [PubMed: 18661994]
29. Giovambattista N, Rossky PJ, Debenedetti PG. J. Phys. Chem. B. 2009; 113 accepted.
30. Pereira B, Jain S, Garde S. J. Chem. Phys. 2006; 124:074704.
31. Beck, TL.; Paulaitis, ME.; Pratt, LR. The potential distribution theorem and models of molecular solutions. Cambridge University Press; 2006.
32. Frenkel, D.; Smit, B. Understanding Molecular Simulations: From Algorithms to Applications. 2nd. New York: Academic Press; 2002.
33. Chandler, D. Introduction to Modern Statistical Mechanics. Oxford University Press; 1987.
34. Zangi R, Berne BJ. J. Phys. Chem. B. 2008; 112:8634–8644. [PubMed: 18582012]
35. Patel AJ. Faraday Disc. 2009; 141:313–315. A preliminary account has been published as a discussion comment.
36. Berendsen HJC, Grigera JR, Straatsma TP. J. Phys. Chem. 1987; 91:6269–6271.
37. Plimpton SJ. J. Comp. Phys. 1995; 117:1–19.
38. Bolhuis PG, Chandler D. J. Chem. Phys. 2000; 113:8154–8160.
39. Miller T, Vanden-Eijnden E, Chandler D. Proc. Nat. Acad. Sci. 2007; 104:14559–14564. [PubMed: 17726097]
40. Jorgensen WL, Madura JD, Swenson CJ. J. Am. Chem. Soc. 1984; 106:6638–6646.
41. Weeks J, Chandler D, Andersen H. J. Chem. Phys. 1971; 54:5237–5247.
42. Ferrenberg AM, Swendsen RH. Phys. Rev. Lett. 1989; 63:1195–1198. [PubMed: 10040500]
43. Kumar S, Rosenberg JM, Bouzida D, Swendsen RH, Kollman PA. J. Comp. Chem. 1992; 13:1011–1021.
44. Souaille M, Roux B. Computer Phys. Comm. 2001; 135:40–57.
45. Before integrating the joint distribution, $P_V(N;\tilde{N})$, it is important to ensure that the conditional probability distribution, $P_V(\tilde{N}|N)$ has been sampled adequately for the entire range of relevant $\tilde{N}$ values. Failure to do so can result in significant errors in $P_V(N)$.We have circumvented this problem by choosing a small value of ξ = 0:1Å, so that $\tilde{N}$ closely follows N.
46. Estimates of statistical uncertainties in our results were obtained by employing WHAM for 8 sets of simulation data and calculating the standard deviation of the reported variable.
47. The data for thin and cubic volumes end at different values of the reduced fluctuation because their standard deviations, $\sqrt{\langle(\delta N)^2\rangle_V}$, differ by 18% despite the fact that their distributions have the same mean, $\langle N\rangle_V = \rho v$. This difference reflects that $\langle(\delta N)^2\rangle_V = \rho v + \rho^2 \int_V d\mathbf{r} \int_V d\mathbf{r}' [g(|\mathbf{r}-\mathbf{r}'|)-1]$, where the bulk solvent radial distribution function, $g(r)$, oscillates about its asymptotic value of 1.
48. Vega C, de Miguel E. J. Chem. Phys. 2007; 126:154707. [PubMed: 17461659]
49. Huang DM, Geissler PL, Chandler D. J. Phys. Chem. B. 2001; 105:6704–6709.
50. Non-Coulombic interactions in the SPC-E model are truncated in our simulations at 10Å. Corrections to this truncation affect the surface tension by less than 5%, which is within uncertainties of the reported values of the surface tension.48,49
51. As an estimate of the expected difference between γ and γ, consider the curvature correction for a spherical solute of the same volume (1728Å^3) as the probe volumes. Assuming the Tolman length to be 0:9Å for a sphere of radius 7.44Å,49 one finds $\gamma \approx 0.76\gamma$.

NIH-PA Author Manuscript

NIH-PA Author Manuscript

NIH-PA Author Manuscript

52. If t is the thickness of the probe volume and s is the side of the square cross-section, all probe volumes v referred to in Fig. 2b have size, $s^2t = 1728\text{Å}^3$ and a surface area, $A_v = 2s^2 + 4st$.
53. Since $P_{\delta v}(N)$ is a gaussian distribution with mean, $\langle N\rangle_{\delta v}$, and variance, $\langle(\delta N)^2\rangle_{\delta v}$, the distribution for the sum of waters in the n independent δv volumes, $P_{n\delta v}(N)$, is also gaussian with mean, $\langle N\rangle_{n\delta v} = n\langle N\rangle_{\delta v}$, and variance, $\langle(\delta N)^2\rangle_{n\delta v} = n\langle(\delta N)^2\rangle_{\delta v}$.
54. The values of $\sqrt{\langle(\delta N)^2\rangle_v}$ vary somewhat depending on the probe volume being considered. For the cubic v, it is 3.12, for the thin v, it is 3.68 and for nδv, it is 4.34.47
55. Bramwell ST, Fortin J-Y, Holdsworth PCW, Peysson S, Pinton J-F, Portelli B, Sellitto M. Phys. Rev. E. 2001; 63:041106.
56. Huang DM, Chandler D. Phys. Rev. E. 2000; 61:1501–1506.
57. Willard AP. Faraday Disc. 2009; 141:309–313.
58. Choudhury N. J. Phys. Chem. B. 2008; 112:6296–6300. [PubMed: 18442285]

NIH-PA Author Manuscript

NIH-PA Author Manuscript

NIH-PA Author Manuscript

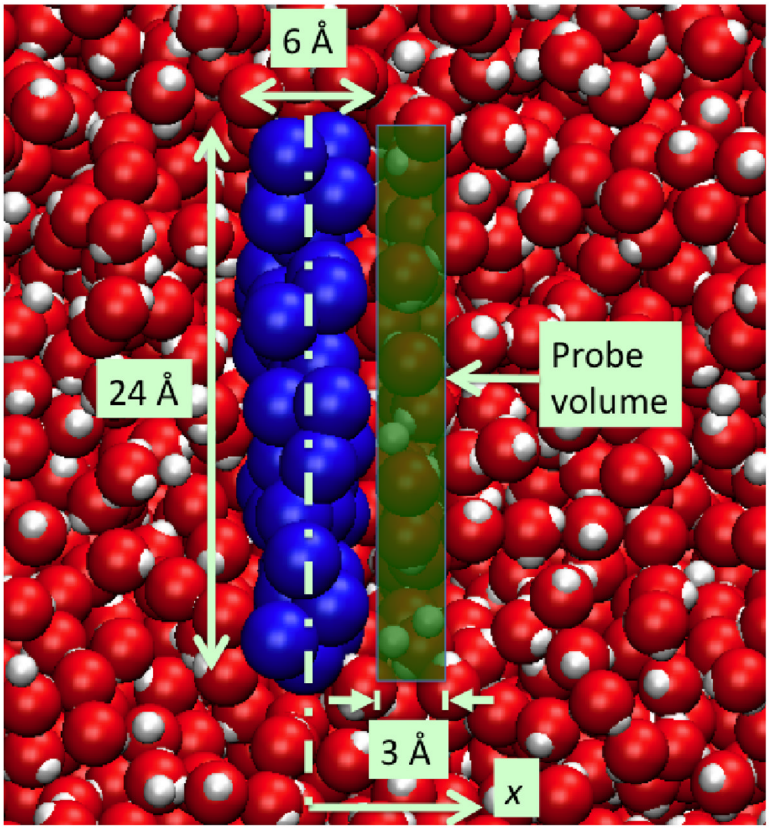

Figure 1.
A typical probe volume, v = (3 × 24 × 24) Å^3, is shown here adjacent to a hydrophobic surface (blue particles). The rendered water molecules (red and white) are in a typical equilibrium configuration taken from one of our simulations.

NIH-PA Author Manuscript
NIH-PA Author Manuscript
NIH-PA Author Manuscript

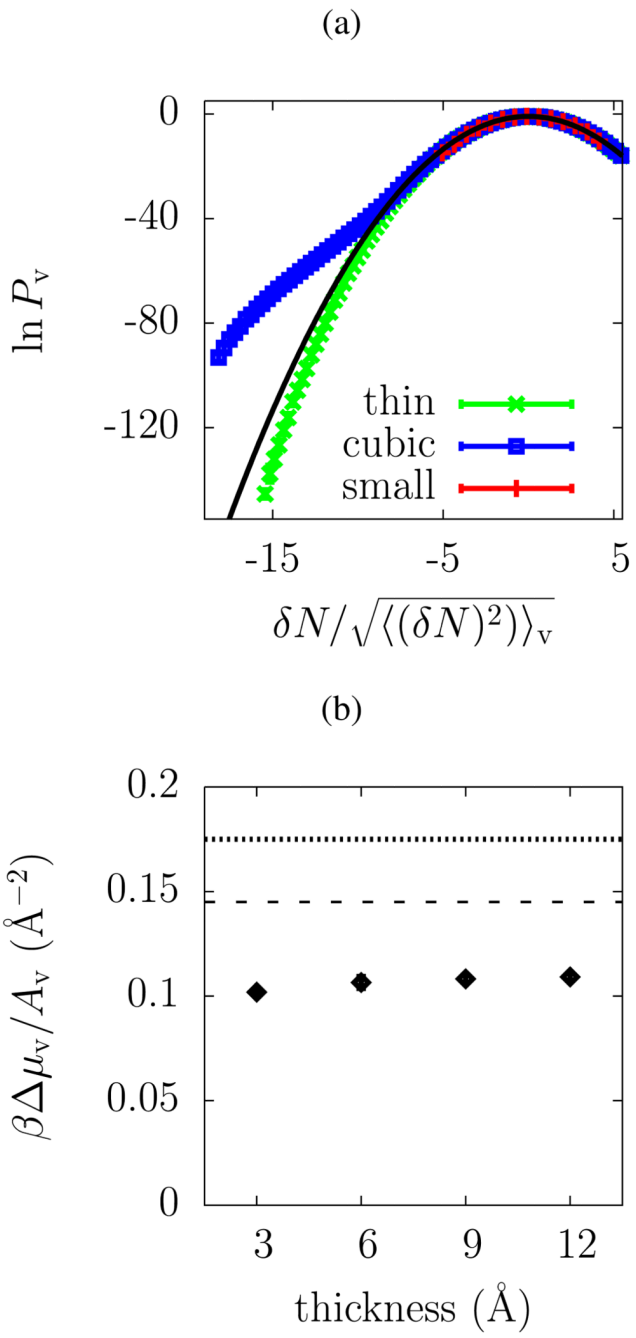

Figure 2.

(a) Probability distribution of finding N water oxygens in a probe volume v in bulk water for a "small" cubic v = (6 × 6 × 6) Å^3, a larger "cubic" v = (12 × 12 × 12) Å^3 and a "thin" v = (3 × 24 × 24) Å^3.47 The solid line refers to the Gaussian distribution with the same mean and variance; $\delta N = N - \langle N\rangle_v$, where $\langle N\rangle_v = \rho v$ is the mean number of oxygen centers in the probe volume v. (b) The solvation free energy, $\Delta\mu_v$, in units of k_BT, per unit surface area, A_v, for probe cavities with different thicknesses and square cross-sections, but the same large volume [(12Å)^3 = 1728Å^3]. The dashed48 and the dotted49 lines indicate reported values of the the surface tension of SPC-E water.50,51 For both (a) and (b), statistical error estimates for our simulation results are smaller than the size of the symbols used.

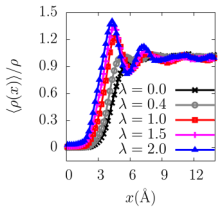

Figure 3.
Mean water density $\langle\rho(x)\rangle$, relative to its bulk liquid value, ρ, perpendicular to extended hydrophobic solutes with different strengths of solute-solvent attractions, λ.

NIH-PA Author Manuscript
NIH-PA Author Manuscript
NIH-PA Author Manuscript

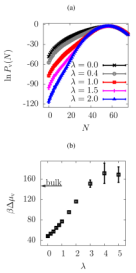

Figure 4.

(a) $P_v(N)$ for probe volumes v = (3 × 24 × 24) Å^3 adjacent to hydrophobic solutes with different attractive solute-solvent couplings, λ. (b) The corresponding solvation free energies for the empty volume v. The arrow shows the value of this free energy when the probe volume is placed in bulk rather than adjacent to the solute. The error bars on the last three points in (b) are standard deviation error estimates for the simulation results for the free energy. Error estimates for all other results shown in both (a) and (b) are smaller than the symbols used.

NIH-PA Author Manuscript
NIH-PA Author Manuscript
NIH-PA Author Manuscript

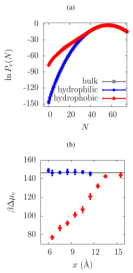

Figure 5.

(a) $P_v(N)$ for v = (3 × 24 × 24) $Å^3$ in bulk, adjacent to the hydrophilic solute, and adjacent to the hydrophobic solute with solute-solvent attraction parameter λ = 1. (b) The change in solvation free energies of the probe volume v at different parallel positions from the solutes.

NIH-PA Author Manuscript NIH-PA Author Manuscript NIH-PA Author Manuscript